fractal and fractional

MDPI

Article

Fractal Evolution Characteristics of Pore Structure in Coal-Acidified Stimulation

Dan Zhou [1,2,3,*], Zhiqiang Lv [1,2,3], Yunxing Cao [1,2,3,*], Gaofeng Liu [1,2,3], Xinsheng Zhang [2,3,4], Bin Shi [1,2,3], Junsheng Zhang [1,2,3] and Shimin Liu [5]

1 School of Resources & Environment, Henan Polytechnic University, Jiaozuo 454003, China; 18336589926@163.com (Z.L.); liugaofeng82@163.com (G.L.); shibinwen-ls@163.com (B.S.); zhangjunsheng2008@163.com (J.Z.)
2 Collaborative Innovation Center of Coal Work Safety and Clean High Efficiency Utilization, Henan Polytechnic University, Jiaozuo 454003, China; zhangxswei@163.com
3 Henan International Joint Laboratory for Unconventional Energy Geology and Development, Jiaozuo 454003, China
4 School of Civil Engineering, Henan Polytechnic University, Jiaozuo 454003, China
5 Department of Energy and Mineral Engineering, G3 Center and Energy Institute, Pennsylvania State University, University Park, PA 16802, USA; szl3@psu.edu
* Correspondence: 18639180517@163.com (D.Z.); yxcao17@126.com (Y.C.)

Abstract: The pore structure and connectivity of coal are the primary factors influencing the permeability of coal reservoirs. However, clay and carbonate minerals are commonly found filling the pores and fractures within coal. To address the impact of these minerals on fracturing effectiveness, acidic fracturing technology has been introduced. This technique has proven to be an effective measure for enhancing the extraction rate of low-permeability coal seams with high mineral content. In this study, coal samples were treated with a 3% HCl solution, and the changes in the pore structure of the coal before and after acidification were analyzed through low-temperature nitrogen adsorption and X-ray diffraction (XRD) testing. The results were as follows: After acidification, the specific surface area, total pore volume, pore volume in different stages, and average pore size of the coal samples all significantly increased. Specifically, the BET specific surface area grew by an average of 4.8 times and the total pore volume expanded by an average of 7.7 times, with the pore volumes in the pore size ranges of <10 nm and 10–60 nm increasing by an average of 10.1 times and 7.7 times. The smoothness of the pore surface and connectivity of the pore structure in the coal samples improved, as indicated by decreased fractal dimensions D_1 (reflecting pore surface roughness) and D_2 (representing pore size distribution uniformity). The acidification mechanism was mainly attributed to the dissolution of carbonate minerals in the coal, which led to the removal of obstructive minerals such as ankerite and calcite that had accumulated in the coal pores. This resulted in the formation of new micropores and microfractures, achieving pore volume enhancement and pore expansion.

Keywords: coal; acidification; pore structure; permeability enhancement; coalbed methane; mineral

check for updates

Academic Editor: Alex Elías-Zúñiga

Received: 29 December 2024
Revised: 19 January 2025
Accepted: 20 January 2025
Published: 22 January 2025

Citation: Zhou, D.; Lv, Z.; Cao, Y.; Liu, G.; Zhang, X.; Shi, B.; Zhang, J.; Liu, S. Fractal Evolution Characteristics of Pore Structure in Coal-Acidified Stimulation. *Fractal Fract.* **2025**, *9*, 62. https://doi.org/10.3390/fractalfract9020062

Copyright: © 2025 by the authors. Licensee MDPI, Basel, Switzerland. This article is an open access article distributed under the terms and conditions of the Creative Commons Attribution (CC BY) license (https://creativecommons.org/licenses/by/4.0/).

1. Introduction

Coalbed methane (CBM) is an important component of unconventional natural gas resources. Developing CBM resources is conducive to improving the energy consumption structure, reducing carbon emissions, and ensuring safe and efficient coal production [1,2]. However, the complexity and low permeability of coal reservoirs in China pose severe

challenges to efficient CBM development. Without the application of permeability enhancement measures to coal reservoirs, CBM wells basically yield no or very low production. Hydraulic fracturing is the primary method for enhancing the permeability of coal reservoirs. Nevertheless, due to the widespread presence of clay and carbonate mineral fillings in coal pores and fractures, the water lock effect often occurs after fracturing, resulting in a decrease in reservoir permeability and production [3–5]. To address the impact of minerals on fracturing effectiveness, acid fracturing was proposed initially and mainly to enhance oil and gas production from carbonate reservoirs in the initial period [6–8]. In the 1960s, acidification began to be adopted in coal seam permeability enhancement experiments, and in recent years, this technology has become an effective measure to improve the extraction efficiency of low-permeability and high-mineral-content coal seams [9–13].

Acid fracturing promotes CBM extraction via the following mechanism: The acid solutions injected into the coal seams react chemically with the minerals in the coal. The reactions dissolve these minerals and widen and clear the coal pores and fracture channels, thereby raising the flowability and recovery rate of CBM. Commonly used acids include hydrochloric acid, nitric acid, sulfamic acid, hydrofluoric acid, formic acid, and acetic acid. Numerous scholars have conducted in-depth studies on the mechanism of interaction between the acid solutions and coal reservoirs during acidization, including chemical reactions, changes in pore and fracture structures, and adsorption–desorption characteristics. They generally believe that acidification can effectively remove most of the minerals in coal, expand the pore volume and porosity in coal, promote the connectivity of the pores, increase the average size of the pores, and enhance coal permeability [3,14–21]. Some studies concluded that acidification can also affect the surface functional groups and chemical structural parameters of coal, thereby breaking down large coal molecules into smaller compounds [22–24]. Acidification can reduce the saturated adsorption capacity of coal and promote CBM desorption, which helps shorten the desorption time of coal [25–28]. The study by Wang et al. showed that acidification can accelerate the oxidation reactions of coal and explained the oxidation mechanisms of coal treated with different acids from a molecular perspective [29]. Additionally, acidification can increase the percentage of hydrophilic groups in coal, thus enhancing its wettability [30,31]. In terms of the impact of acidification on pore structure, Ni et al. demonstrated that wedge-shaped pores in coal can expand into cylindrical pores after nitric acid treatment [32]. Su et al. reported that using multi-component acids such as organic acids and low-concentration inorganic acids can severely disrupt the surface structure of coal particles and induce the generation of numerous cracks and pores [33]. Yu et al. used acetic acid at the 75% concentration to treat cylindrical coal samples and found that acetic acid dissolves minerals rapidly initially and then slowly later, indicating its potential to modify coal reservoir pores and fractures [34]. Combining acidification treatment with other production enhancement measures may yield better acidification effects. According to Lu et al., microwave-assisted hydrochloric acidification is more conducive to acid solution penetration into microfractures and micropores and facilitates the transition of micropores into mesopores and macropores [35]. Mohsen et al. found that the combination of acidification and nitrogen hydraulic fracturing can create a more pronounced fracture network, and a 3% hydrochloric acid concentration can lead to an ideal demineralization effect [36]. Although acidification treatment can increase coal porosity and promote gas flow, it may also lower the compressive strength and elastic modulus of coal due to the dissolution of minerals by the acid solutions [37,38]. This may intensify the sensitivity of coal reservoirs to stress and exert a negative impact on CBM production [39]. Currently, experimental studies on coal seam acidification for permeability enhancement are plentiful, but those on field acidification engineering practices are relatively lacking. Farrokhrouz et al. reported that compared with traditional hydraulic

fracturing, the average mixed flow rate of gas extraction from boreholes can increase by 2–3 times after acid fracturing [40,41]. Wang et al. reported on the application of composite hydrochloric acid and sulfamic acid volume fracturing technology to deep CBM wells; the application was found to achieve considerable gas production, but further optimization of the acid solution concentration is still needed to achieve better fracturing effects [42].

Coal is a typical porous medium whose pore structure directly affects the adsorption and migration of CBM. Previous research has mainly focused on changes in the pore structure parameters of acidized coal, including pore size, pore volume, and specific surface area. However, the complexity and heterogeneity of the coal pore structure after acidification have not been fully elucidated, making the clarification of the fundamental effects and mechanisms of acidification on coal pores impossible. Previous studies have shown that fractal theory can be used to quantitatively characterize the complexity and heterogeneity of pore structure [43–46]. The mineral content in coal positively correlates with its pore fractal dimension [14]. Different types of acid solutions exhibit variations in fractal dimension changes after acidification [38]. Some studies have concluded that both pore surface fractal dimension D_1 and pore structure fractal dimension D_2 decrease after acidification [47], while other studies have pointed out that after acidification, fractal dimension D_1 increases while D_2 decreases [19,35]. Therefore, exploring the evolution laws of fractal dimensions D_1 and D_2 of coal pore structure under acidification is beneficial for providing a more comprehensive and in-depth understanding of the effects and mechanisms of acid solutions on coal porosity.

In summary, coal reservoir acidification shows promise for application in CBM development. Due to the large differences in mineral composition and physical properties among different coal reservoirs, appropriate acid solution systems and concentrations should be selected based on specific coal reservoir characteristics to achieve good acidification and permeability enhancement effects. In this study, lean coal was taken as the research object, and a hydrochloric acid solution with a concentration of 3% was selected for acidification treatment of the coal samples. By performing low-temperature nitrogen adsorption experiments and XRD tests, the evolution characteristics of the coal pore structure before and after acidification were quantitatively studied and the mechanism of acidification behind alterations in the coal pore structure was revealed under pore fractal theory. The results are of great significance for enriching the theory of coal reservoir acidification and can provide a scientific basis and methodological reference for increasing CBM reservoir production through acidification.

2. Experiments

2.1. Preparation and Treatment of Coal Samples

Experimental coal samples were taken from the 3# coal seam in Yuwu Coal Mine in Shanxi Province, China. The coal type was Meager-lean coal. The maximum reflectance of vitrinite, $R_{o,\,max}$, ranged from 2.13% to 2.28%. The volatile content of floating coal ranged from 9.34% to 21.89%. The mineral content varied from 4.4% to 11.5%, with an average of 7.9%. To ensure the accuracy of the experimental results, three powdered coal samples with particle sizes of 60–80 meshes were prepared for low-temperature nitrogen adsorption experiments and three powdered coal samples with particle sizes of 200 meshes were prepared for mineral content tests.

2.2. Low-Temperature Nitrogen Adsorption Experiment

Low-temperature nitrogen adsorption experiments were performed to determine the pore structure of the coal and the coal samples were numbered DW1, DW2, and DW3. The tests were conducted with the aid of an *ASAP2460* surface area and porosity analyzer

according to the *GB/T 21650.3-2011* [48], standard for determining the pore size distribution and porosity of solid materials using the mercury intrusion method and gas adsorption method. The specific procedure was as follows: The prepared coal samples were subjected to low-temperature nitrogen testing first and then immersed in a hydrochloric acid solution with a concentration of 3% for 2 h; finally, they were rinsed and soaked repeatedly with distilled water until the pH value of the distilled water returned to 7. After being filtered out with filter paper, the coal powder was dried in an oven at 60 °C for 8 h and subjected to low-temperature nitrogen testing again.

2.3. XRD Tests

XRD tests were conducted to analyze the changes in mineral content in the coal before and after acidification. The test instrument used was a *Rigaku TTRIII* multifunctional X-ray diffractometer. According to the *SY/T 5163-2018* [49], standard for XRD analysis on clay minerals and common non-clay minerals in sedimentary rocks, the prepared 200-mesh coal powder was first tested using XRD. Subsequently, the tested coal powder was immersed in a hydrochloric acid solution with a concentration of 3% for 2 h and then repeatedly washed with distilled water. After that, the coal powder was filtered through filter paper and dried, before being subjected to XRD testing again.

2.4. Calculation of Pore Fractal Dimension

Based on the results of the low-temperature nitrogen adsorption pore structure tests, the fractal characteristics of the pore structure before and after acidification were quantitatively analyzed via the fractal dimension. In this study, the pore fractal dimension of coal was calculated using the convenient and widely used *Frenkel–Halsey–Hill* (FHH) model. The calculation equations are introduced below.

The FHH model suggests that in the low-pressure stage, nitrogen adsorption by coal is a monomolecular layer adsorption behavior controlled by Van der Waals force at the gas–solid interface. The fractal dimension can be calculated as follows (Equation (1)):

$$ln(V/V_m) = C_1 + [(D-3)/3] * [ln(ln(P_0/P))] \quad (1)$$

In the high-pressure stage, Van der Waals force at the gas–solid interface can be neglected compared with the surface tension at the gas–liquid interface. In this case, the adsorption capacity of coal to nitrogen gas is mainly controlled by the surface tension at the gas–liquid interface. The fractal dimension can be calculated as follows (Equation (2)):

$$ln(V/V_m) = C_2 + (D-3) * [ln(ln(P_0/P))] \quad (2)$$

where V is the gas adsorption volume; V_m is the total gas adsorption capacity; P is the system equilibrium pressure; C_1 and C_2 are curve fitting constants; D is the fractal dimension; and P_0 is the saturation vapor pressure of the adsorbed gas. The value of D is determined from the slope of the line plotted on the basis of the linear correlation between $ln(ln(P_0/P))$ and lnV.

3. Results and Discussion

3.1. Pore Size Distribution

The results of the low-temperature nitrogen adsorption tests on the pore structure of the coal samples before and after acid treatment are presented in Table 1. Overall, the specific surface area, total pore volume, pore volume in different stages, and average pore size of the coal samples significantly increased after acid treatment compared with those before acidification.

Table 1. Results of low-temperature nitrogen adsorption tests on the pore structure of coal samples before and after acid treatment.

Sample	BET Specific Surface Area (m^2/g)	BJH Total Pore Volume (10^{-3} cm^3/g)	BJH Average Pore Diameter (nm)	Pore Volume in Different Stages (10^{-3} cm^3/g)	
				<10 nm	10–60 nm
DW1	0.2089	0.717	12.0612	0.1794	0.538
DW1-HCl	1.1938	5.16	9.1866	3.0847	2.0751
DW2	0.2493	0.787	10.1304	0.2435	0.5435
DW2-HCl	1.1299	5.773	11.4592	1.7061	4.0665
DW3	0.268	0.813	10.764	0.2418	0.5708
DW3-HCl	1.1136	7.063	13.0864	1.5076	5.5555

BET (Brunauer–Emmett–Teller) is a widely used technical method for measuring the surface area of solids. The result of BET for measuring the specific surface area was as follows: Before acidification, this parameter ranged from 0.2089 m^2/g to 0.268 m^2/g, with an average of 0.242 m^2/g. After acidification, it ranged from 1.1136 m^2/g to 1.1938 m^2/g, with an average increase of 1.1458 m^2/g, marking an increase of 4.2–5.7 times and 4.8 times on average.

The BJH (Barrett–Joyner–Halenda) method is a technique used for describing the pore size distribution in porous materials. The result of BJH for measuring the total pore volume was as follows: Before acidification, this parameter ranged from 0.717 $\times$ 10^{-3} cm^3/g to 0.813 $\times$ 10^{-3} cm^3/g, with an average of 0.772 $\times$ 10^{-3} cm^3/g. After acidification, it ranged from 5.16 $\times$ 10^{-3} cm^3/g to 7.063 $\times$ 10^{-3} cm^3/g, with an average increase of 6.0 $\times$ 10^{-3} cm^3/g, indicating an increase of 7.2–8.7 times and 7.7 times on average. The pore volume at different stages was as follows: The test results from using the BJH method demonstrate that the average pore size of all the coal samples lies between 2 nm and 60 nm before and after the acid treatment (Figures 1 and 2). With reference to Hodot's (1961) decimal pore size classification, the pore volume was divided into two stages by taking 10 nm as the boundary. For pores smaller than 10 nm (micropores), before acidification, the pore volume ranged from 0.1794 $\times$ 10^{-3} cm^3/g to 0.2435 $\times$ 10^{-3} cm^3/g, with an average of 0.222 $\times$ 10^{-3} cm^3/g. After acidification, it ranged from 1.5076 $\times$ 10^{-3} cm^3/g to 3.0547 $\times$ 10^{-3} cm^3/g, with an average of 2.099 $\times$ 10^{-3} cm^3/g, recording an increase of 6.2–17.2 times and 10.1 times on average. For pores between 10 nm and 60 nm (in comparison to small pores), before acidification, the pore volume ranged from 0.538 $\times$ 10^{-3} cm^3/g to 0.5708 $\times$ 10^{-3} cm^3/g, with an average of 0.551 $\times$ 10^{-3} cm^3/g. After acidification, it ranged from 2.0751 $\times$ 10^{-3} cm^3/g to 5.5555 $\times$ 10^{-3} cm^3/g, with an average of 3.9 $\times$ 10^{-3} cm^3/g. The increase brought on by acidification was 3.0–9.2 times, averaging an increase of 7 times.

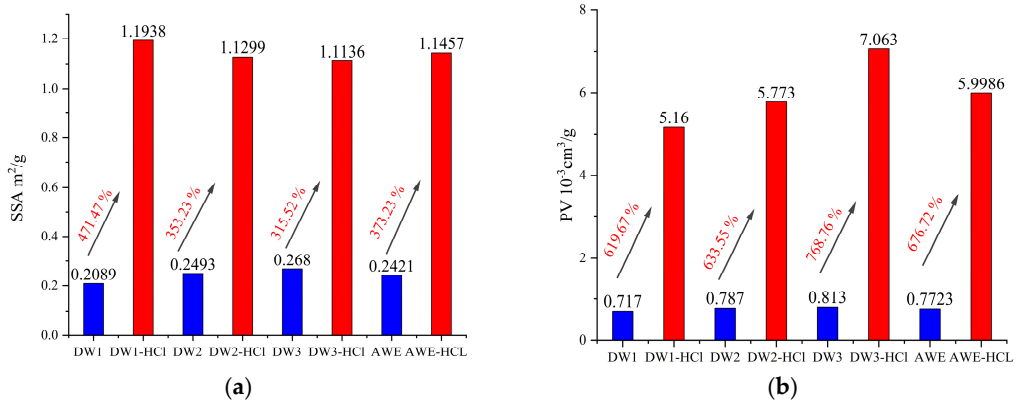

Figure 1. Distribution characteristics of the pore structure before and after acidification. (**a**) The trend of changes in a specific surface area. (**b**) The trend of changes in the average pore volume.

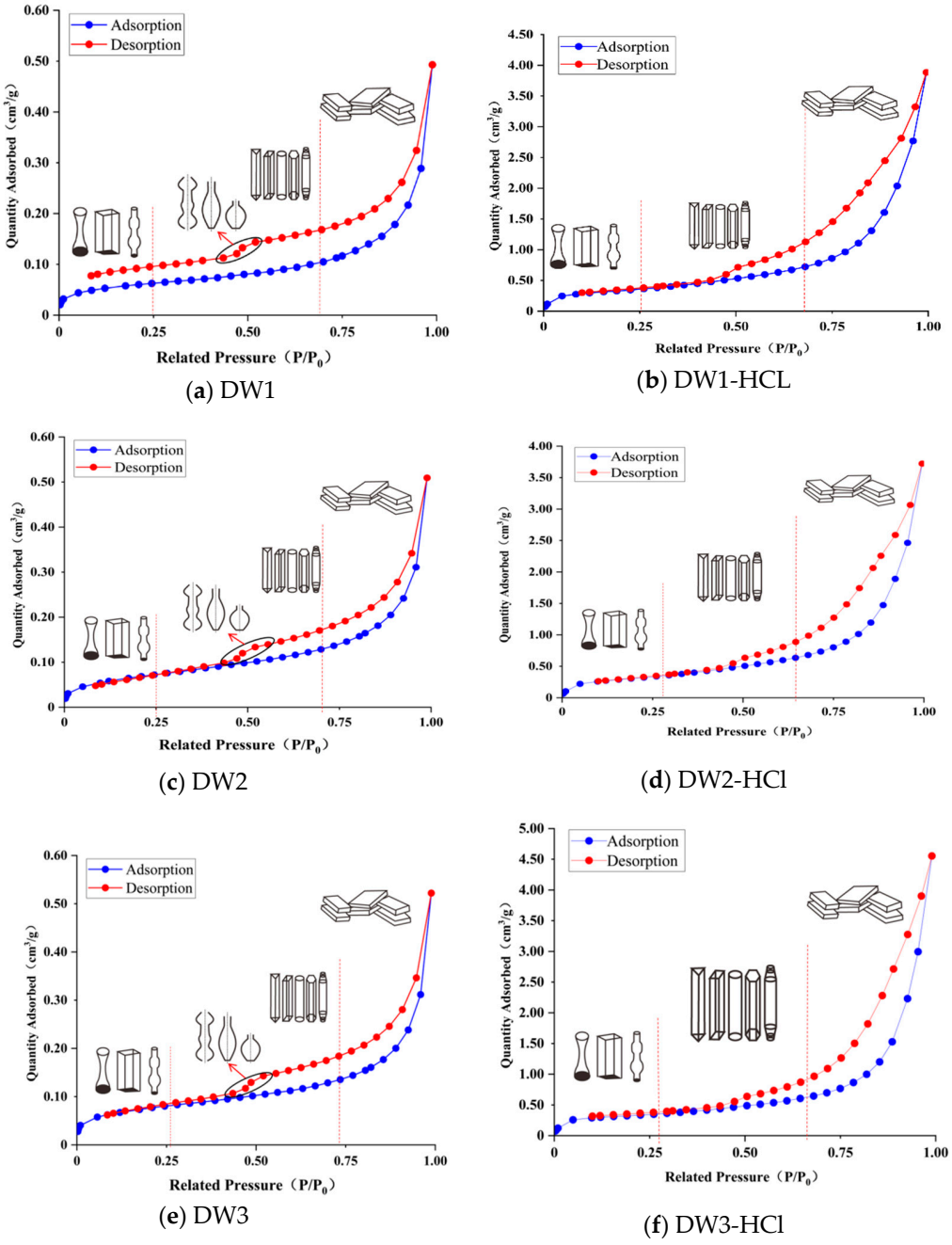

Figure 2. Low-temperature nitrogen adsorption curves of coal samples before and after acidification.

The average pore radius measured by BJH was as follows: Except for the DW1 coal sample, which showed a decrease in average pore radius, the other two coal samples, DW2 and DW3, exhibited an increasing trend after acidification. Specifically, their average pore sizes increased from 10.1304 to 10.764 nm before acidification to 11.459–13.0864 nm after acidification (DW2-HCl and DW3-HCl), a 12.9–21.5% increase. According to the statistical data in Table 1 and Figure 1, the increase in the micropore (smaller than 10 nm) volume of the DW1 sample after acidization was much greater than those of the DW2 and DW3 samples, while the increase in small pore volume was far smaller than that of the DW2 and DW3 samples, which may be a direct factor in the average pore size of the DW1 coal sample decreasing after acidification. The fundamental reason behind this decrease lies in the differences in the pore structure of the original coal sample itself. After acidification, a

large number of micropores that were originally filled with minerals or that maintained a closed state opened up.

3.2. Nitrogen Adsorption and Desorption Isotherms

The low-temperature nitrogen adsorption and desorption curves reflect the pore structure and connectivity of coal. As presented in Figure 2, the low-temperature nitrogen adsorption curves of all coal samples exhibit a type II pattern. That is, the first half is convex and increases gradually, while the second half surges sharply. Such a pattern results from the transition from nitrogen molecule monomolecular layer adsorption to nitrogen molecule multimolecular layer adsorption and then to capillary condensation, which is indicative of relatively intact continuity in the pore structure of the coal. The adsorption and desorption curves form obvious hysteresis loops both before and after acidification and the shape of these hysteresis loops can reflect the morphology of the pore structure. To be specific, for the DW-1 sample, before acidification, the adsorption and desorption curves do not close, indicating that the adsorbed nitrogen gas fails to completely desorb from the coal surface; that is, desorption is difficult. Furthermore, the desorption curve bends suddenly near a relative pressure (P/P_0) of 0.5 (Figure 2a), which suggests that the pore structure is dominated by narrow-neck-shaped, plate-shaped, and ink-bottle-shaped pores. After acidification, the adsorption and desorption curves close, and the desorption curve bends gradually near a relative pressure (P/P_0) of 0.5 (Figure 2b), which marks a transformation to another pore type, mainly to conical and cylindrical pores. For the DW-2 and DW-3 samples, before acidification, the curves close, and the desorption curves also exhibit a sudden bend near a relative pressure (P/P_0) of 0.5 (Figure 2c,e). After acidification, the desorption curves also bend gradually near a relative pressure (P/P_0) of 0.5 (Figure 2d,f). In terms of the hysteresis loop shapes before and after acidification, the curves for the three coal samples evolve into a consistent pattern, reflected by the transformation of the pore morphology from narrow-neck-shaped, plate-shaped, and ink-bottle-shaped pores to conical and cylindrical pores. These results imply that acid dissolution contributes to increasing the pore volume and expanding the pore size.

3.3. Pore Fractal Characteristics

As revealed in fractal theory, the fractal dimension of the pore structure of coal holds fractal significance only when it falls within the range of 2–3. The pore fractal dimension calculated using Equation (1) is smaller than 2, which is obviously inconsistent with the objective fact of pore fractal, whereas the pore fractal dimension calculated using Equation (2) falls within the range of 2–3. Therefore, Equation (2) is adopted to calculate the pore fractal dimension. As depicted in Figure 3, the relationship curves between $ln(ln(P_0/P))$ and lnV before and after acidification can both be divided into two segments: $P/P_0 < 0.5$ and $P/P_0 > 0.5$, corresponding to two fractal dimensions, D_1 and D_2, respectively. D_1 is typically used to reflect the roughness of the pore surface, with a larger D_1 representing a rougher pore surface. D_2 is used to reflect the uniformity of pore size distribution, with a larger D_2 denoting a more uneven pore size distribution.

The pore fractal dimensions of coal before and after acidification are listed in Table 2. Fractal dimension D_1 ranges from 2.0263 to 2.4167, and D_2 varies from 2.3904 to 2.6012. The fit correlation coefficient, R^2, is greater than 0.9, which means that the use of fractal dimensions for a quantitative study on the evolution characteristics of pore structure before and after acidification is reliable. As can be seen from Figure 4 and Table 2, after acidification, the fractal dimensions D_1 and D_2 of all coal samples noticeably decrease by 20–34%. Previous research has shown that a larger fractal dimension signifies a more complex pore structure, a rougher pore surface, narrower pore throats, and poorer con-

nectivity, and some studies have shown that the removal of minerals and organic matter in coal can simplify the pore structure and reduce the D_2 fractal dimension of the pore structure. The pore test results in this study show that both fractal dimensions D_1 and D_2 decrease after acidification, implying that acid treatment can smoothen the pore surface of coal, uniformize the pore size distribution, and enhance the connectivity. This finding agrees with the pore distribution characteristics measured in the low-temperature nitrogen adsorption experiments, as well as the pore morphology evolution characteristics reflected by the low-temperature nitrogen adsorption and desorption curves.

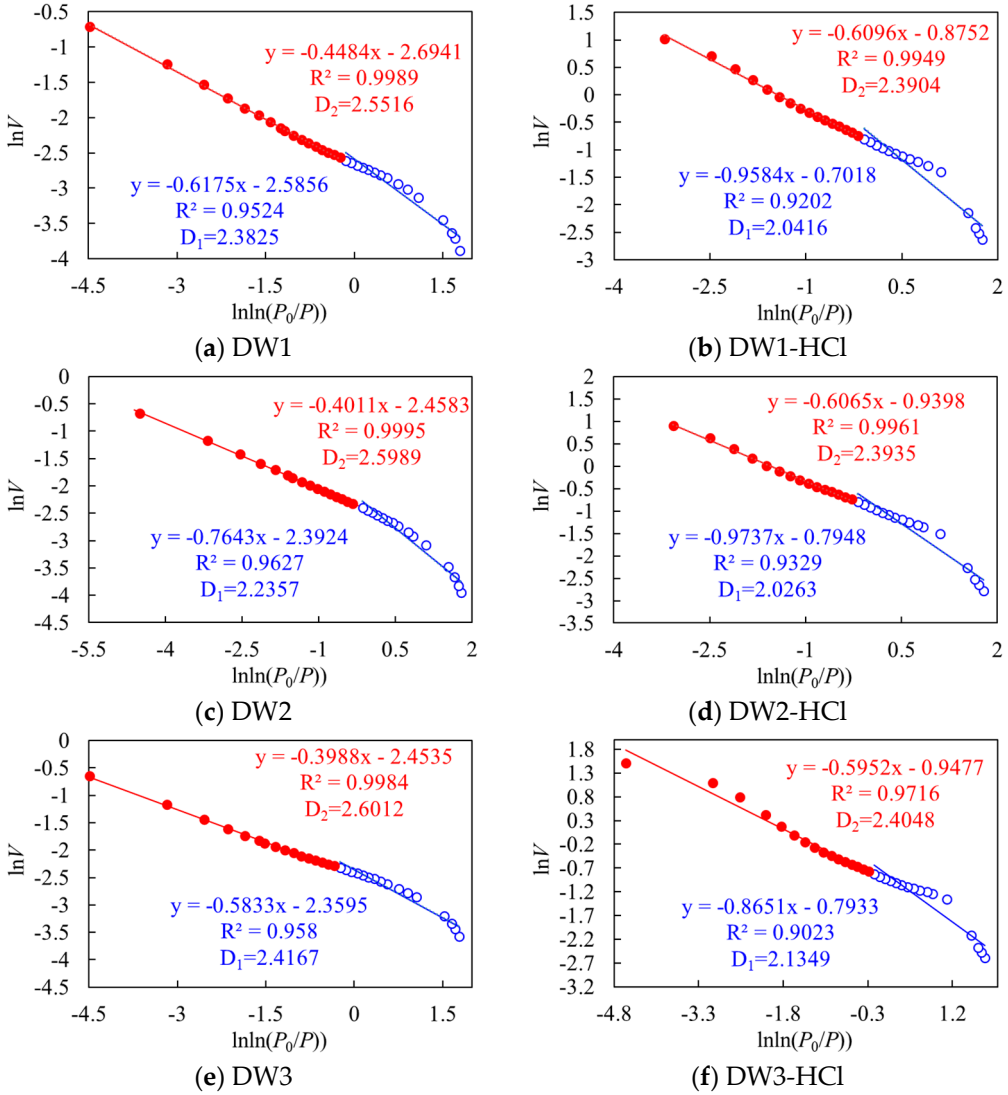

Figure 3. Fractal dimension changes in the acidized coal samples.

Table 2. Fractal dimensions of the coal samples.

Sample	D_1	R^2	D_2	R^2
DW1	2.3825	0.9524	2.5516	0.9989
DW1-HCl	2.0416	0.9202	2.3904	0.9949
DW2	2.2357	0.9627	2.5989	0.9995
DW2-HCl	2.0263	0.9329	2.3935	0.9961
DW3	2.4167	0.958	2.6012	0.9984
DW-3-HCl	2.1349	0.9023	2.4048	0.9716

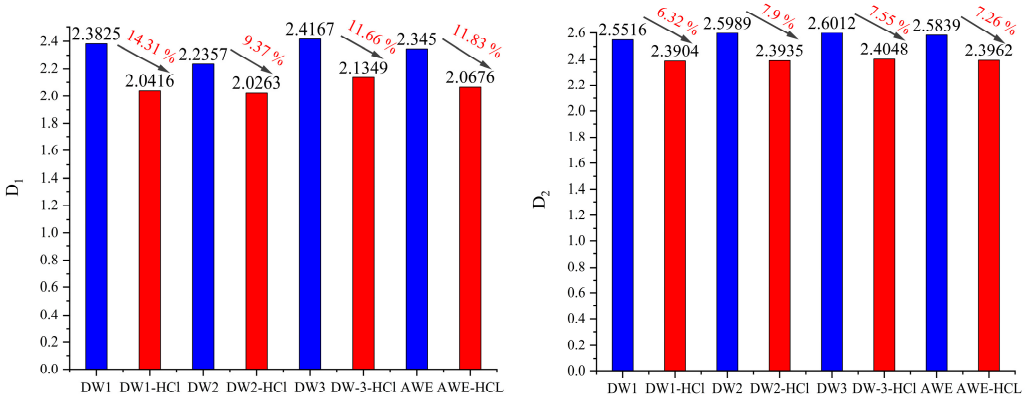

(**a**) (**b**)

Figure 4. Variation trend of the fractal dimensions: (**a**) The trend of changes in D_1. (**b**) The trend of changes in D_2.

3.4. Acidizing Mechanism

As seen in the low-temperature nitrogen adsorption tests, the acidification effect on the internal pore structure of the coal samples is primarily concentrated in three aspects: Firstly, acidification noticeably enlarges the specific surface area, total pore volume, and stage pore volume of the pore structure, by 4–10 times on average. Secondly, acidification facilitates the transformation of the pore morphology from narrow-neck-shaped, plate-shaped, and ink-bottle-shaped pores to conical and cylindrical pores, thereby expanding the seepage channels and enhancing pore connectivity. Lastly, the pore structure improves across a wide range, with changes observed in the entire pore size range (<60 nm). Both fractal dimensions D_1 and D_2 of the pore structures of the coal samples decreased remarkably, by 0.2–0.34.

Previous studies have unveiled that treatment with acidic solutions promotes a dissolution chemical reaction for organic matter or minerals in coal. As the HCl solution constitutes a strongly acidic environment, the obvious changes in coal pore structure can be attributed to acidification-induced dissolution. The XRD test results in Table 3 demonstrate that, after acidization, the proportion of clay minerals in the total mineral content for the three coal samples substantially increases, primarily manifested by the complete disappearance of ankerite and calcite. This observation demonstrates that in a hydrochloric acid solution environment, the minerals in coal primarily undergo the following three chemical reactions:

$$CaCO_3(\text{calcite}) + 2HCl = CaCl_2 + CO_2\uparrow + H_2O$$

$$CaMg(CO_3)_2(\text{dolomite}) + 4HCl = CaCl_2 + MgCl_2 + 2CO_2\uparrow + 2H_2O$$

$$Fe_2O_3(\text{hematite}) + 6HCl = 2FeCl_3 + 3H_2O$$

Table 3. XRD test results for the mineral content in the coal samples.

Coal Sample	Mineral Content (%)			
	Quartz	Calcite	Iron Dolomite	Clay Minerals
DW1	7.6	17.8	28.6	46.0
DW2	/	21.2	25.2	53.6
DW3	/	17.8	21.0	41.2
DW1-HCl	11.8	/	/	88.2
DW2-HCl	/	/	/	100.0
DW-3-HCl	/	/	/	100.0

Note: The data in Table 3 are derived from an analysis on the diffraction data of whole-core mineral crystals, and the amorphous substances in the coal are not included in the calculations. The relative content of amorphous substances can be obtained via the low-temperature ashing method.

The acidification modification technology, unlike other physical coal seam modification technologies, falls within the scope of chemical modification. By enabling chemical dissolution reactions of organic matter or minerals in coal, it dissolves and removes pore-blocking deposits, generates new micropores and microfractures, and achieves capacity enhancement and pore enlargement. Furthermore, the dissolution process not only clears out some of the blockages in the pores and fractures, allowing the pores to be linked together, but also improves the surface smoothness of the pore structure to some extent. These improvements facilitate the formation of favorable channels for the efficient production of gas reservoirs (Figure 5). Hence, the core characteristic of coal seam acid fracturing modification lies in its wide range of modifications for coal sample pore structure and its ability to operate at small pore sizes (as low as on the nanometer scale).

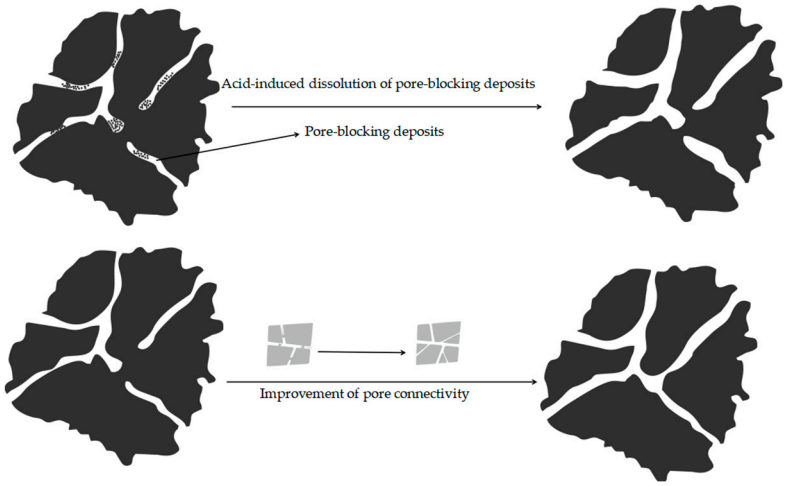

Figure 5. Acidification and dissolution mechanism of pore structures.

This study clarifies the mechanism behind the permeability enhancement and CBM production increase using acid fracturing technology on the microscopic pore structure scale. Essentially, the microscopic pore volume expansion, pore enlargement, and the increase and accumulation of structural quantities ultimately lead to a deterioration in the macroscopic mechanical properties of a coal mass. In summary, coal seam modification via acid fracturing is a multiscale—from the micro scale to the macro scale—cumulative damage and degradation process. The application of acid fracturing to coal seam modification not only addresses the challenges of difficult CBM desorption and poor reservoir permeability at the source but also facilitates the connectivity of multiscale pores and fractures. This connectivity contributes to reducing the fracturing pressure during coal seam modification and expanding the modified fracture volume of the coal seam, ultimately achieving efficient permeability enhancement and CBM production increase.

4. Conclusions

In this study, based on low-temperature liquid nitrogen adsorption experiments and XRD tests, the changes in the pore structure parameters of the Yuwu 3# lean coal samples before and after acidification using a hydrochloric acid solution with a concentration of 3% were analyzed, and the fractal evolution characteristics of the pore structure of the acidized coal sample were elucidated. The main conclusions are as follows:

a. Acidification treatment can modify the pore structure across a wide range, with changes observed in the entire pore size range (<60 nm). After acidification, the specific surface area, total pore volume, and pore volume in different stages of the pore structure in the coal samples all increase markedly, by 4–10 times on average.

b. Acidification can improve the pore size across all of the pore size segments. It not only opens pores filled with minerals through dissolution but also opens originally closed micropores, increasing the effective porosity by 2–3 times. The shapes of the low-temperature nitrogen adsorption and desorption curves indicate that after acidification, the pore morphology of the coal sample tends to transform from narrow-neck-shaped, plate-shaped, and ink-bottle-shaped pores to conical and cylindrical pores. After acidification, the fractal dimension of the pore structure decreases, suggesting that acidification can smoothen the pore surfaces, uniformize the pore size distribution, and enhance the connectivity.

c. This study suggests that the dissolution of carbonate minerals such as ankerite and calcite in coal using hydrochloric acid is the primary reason for the improved connectivity of the pore structure and permeability of coal. When improving the connectivity of the pore structure, acidification acts to "support the weak and enhance the strong". "Supporting the weak" refers to the transformation of the initially disconnected micropores into weakly or even strongly connected pores, while "enhancing the strong" refers to the enhancement in the connectivity of the weakly connected mesoscopic and macroscopic pores and fractures into strongly connected ones. These effects contribute to enhancing the permeability of the coal seam.

d. While acid fracturing technology offers significant advantages in enhancing oil and gas well production and recovery rates, it also has limitations in various aspects, including technical operation complexity, geological condition constraints, environmental impact, and economic cost considerations.

Author Contributions: Conceptualization, D.Z., Y.C. and G.L.; data curation, Z.L., J.Z. and B.S.; formal analysis, Z.L., J.Z., B.S. and Y.C.; funding acquisition, D.Z. and G.L.; methodology, D.Z., G.L. and X.Z.; supervision, D.Z. and Y.C.; visualization, Z.L.; writing—original draft, D.Z., G.L. and X.Z.; writing—review and editing, D.Z. and S.L. All authors have read and agreed to the published version of the manuscript.

Funding: This research was supported by the National Natural Science Foundation of China (no. 42230814, no. 42372204, and no. 42472240), the Henan Province Science and Technology Research Project (no. 242102320365), and the Key Research Project of Higher Education Institutions in Henan Province (no. 24B170005).

Data Availability Statement: The data presented in this study are available from the corresponding author upon request.

Conflicts of Interest: The authors declare no conflicts of interest.

References

1. Liu, G.; Liu, H.; Xian, B.; Gao, D.; Wang, X.; Zhang, Z. Fuzzy pattern recognition model of geological sweetspot for coalbed methane development. *Petrol. Explor. Dev.* **2023**, *50*, 924–933. [CrossRef]
2. Xian, B.; Liu, G.; Bi, Y.; Gao, D.; Li, W.; Yunxing, C.; Shi, B.; Zhang, Z.; Zhang, Z.; Tian, L.; et al. Coalbed methane recovery enhanced by screen pipe completion and jet flow washing of horizontal well double tubular strings. *J. Nat. Gas Sci. Eng.* **2022**, *99*, 104430. [CrossRef]
3. Zhang, Z.; Liu, G.; Cao, Y.; Lin, J.; Jin, Y.; Xian, B.; Lv, R.; Zhang, Z. Experimental Investigation of CS_2 Extraction to Enhance the Permeability of Coal. *Transp. Porous Media* **2021**, *136*, 899–922. [CrossRef]
4. Zhang, M.; Fu, X.; Zhang, Q.; Cheng, W. Research on the organic geochemical and mineral composition properties and its influence on pore structure of coal-measure shales in Yushe-Wuxiang Block, South Central Qinshui Basin, China. *J. Petrol. Sci. Eng.* **2019**, *173*, 1065–1079. [CrossRef]
5. Liu, Z.; Shi, B.; Ge, T.; Sui, F.; Wang, Y.; Zhang, P.; Chang, X.; Liu, Y.; Wang, Y.; Wang, Z. Tight sandstone reservoir sensitivity and damage mechanism analysis: A case study from Ordos Basin, China and implications for reservoir damage prevention. *Energy Geosci.* **2022**, *3*, 394–416. [CrossRef]

6. Gou, B.; Liu, Z.; Zhou, J.; Xu, K.; Xiao, B.; Pu, K.; Guo, J. Experimental and modeling study on the acid-etching and conductivity of hydraulic fractures in carbonate rocks: A critical review. *J. Petrol. Sci. Eng.* **2025**, *245*, 213517. [CrossRef]
7. Li, N.; Dai, J.; Li, J.; Bai, F.; Liu, P.; Luo, Z. Application status and research progress of shale reservoirs acid treatment technology. *Nat. Gas Ind. B* **2016**, *3*, 165–172. [CrossRef]
8. Su, X.; Qi, N.; Lu, Y.; Liu, C.; Liu, X. Experimental study on acid etching mechanism of acid fracturing in carbonate reservoirs. *Geoenergy Sci. Eng.* **2024**, *241*, 213079. [CrossRef]
9. Gan, R.; Zuo, S.J.; Si, J.T.; Liu, C.W.; Tian, F.; Jiang, Z.Z.; Wang, C.W.; Peng, S.Q.; Xu, Z.Y. Effects of Different Concentrations of Weak Acid Fracturing Fluid on the Microstructure of Coal. *Nat. Resour. Res.* **2024**, *33*, 2215–2236.
10. Zhang, B.; Deng, Z.; Fu, X.; Yu, K.; Zeng, F. An experimental study on the effects of acidization on coal permeability: Implications for the enhancement of coalbed methane production. *Energy* **2023**, *280*, 128145. [CrossRef]
11. Balucan, R.D.; Turner, L.G.; Steel, K.M. X-ray μCT investigations of the effects of cleat demineralization by HCl acidizing on coal permeability. *J. Nat. Gas Sci. Eng.* **2018**, *55*, 206–218. [CrossRef]
12. Luo, M.; Cui, S.; Zhou, X.; Li, S.; Fan, C. Experimental study on permeability enhancement of coal seam with high mineral content by acid fracturing. *Energy Source Part A* **2020**, *46*, 7770–7783. [CrossRef]
13. Fan, C.; Luo, M.; Li, S.; Zhang, H.; Yang, Z.; Liu, Z. A Thermo-Hydro-Mechanical-Chemical Coupling Model and Its Application in Acid Fracturing Enhanced Coalbed Methane Recovery Simulation. *Energies* **2019**, *12*, 626. [CrossRef]
14. Li, H.; He, J.; Lu, J.; Lin, B.; Lu, Y.; Shi, S.; Ye, Q. A review of laboratory study on enhancing coal seam permeability via chemical stimulation. *Fuel* **2022**, *330*, 125561. [CrossRef]
15. Zheng, C.; Liu, S.; Xue, S.; Jiang, B.; Chen, Z. Effects of chemical solvents on coal pore structural and fractal characteristics: An experimental investigation. *Fuel* **2022**, *327*, 125246. [CrossRef]
16. Xing, M.; Xu, C.; Zhou, G.; Sun, L.; Du, W. Experimental investigation for effect of multicomponent inorganic-organic acid solution on pore structure of lignite. *Powder Technol.* **2021**, *392*, 503–513. [CrossRef]
17. Li, S.; Ni, G.; Wang, H.; Xun, M.; Xu, Y. Effects of acid solution of different components on the pore structure and mechanical properties of coal. *Adv. Powder Technol.* **2020**, *31*, 1736–1747. [CrossRef]
18. Gao, J.; Fang, Y.; Li, J.; Lu, F.; Hu, J. Influence of multi-component acid acidification on anti-reflection effect of high-rank coal in Zhongmacun Mine. *J. Saf. Environ.* **2022**, *22*, 3119–3126.
19. Wen, Y.; Ni, G.; Zhang, X.; Zheng, Y.; Wang, G.; Wang, Z.; Huang, Q. Fine characterization of pore structure of acidified anthracite based on liquid intrusion method and Micro-CT. *Energy* **2023**, *263*, 125639.
20. Zhao, B.; Wen, G.; Sun, H.; Yang, S. Experimental study on response law of premeability of coal to acidification. *J. China Coal Soc.* **2017**, *42*, 2019–2025.
21. Zhang, Z.; Liu, G.; Wang, X.; Lin, J.; Barakos, G.; Chang, P. Targeted Stimulation of Micropores by CS_2 Extraction on Molecular of Coal. *Molecules* **2024**, *29*, 2993. [CrossRef] [PubMed]
22. Luo, J.; Cai, Y.; Tang, H.; Yu, J.; Zheng, L.; Li, H. Mechanism of the pore and molecular structure evolution of coal exposed to acid mine drainage (AMD). *Sci. Total Environ.* **2024**, *906*, 167836. [CrossRef] [PubMed]
23. Wei, Z.; Lin, B.; Tong, L.; Ting, L.; Wei, Y. Effect of acidification on microscopic properties and pore structure of coal. *Fuel* **2023**, *343*, 127834. [CrossRef]
24. Zhang, Z.; Liu, G.; Chang, P.; Wang, X.; Lin, J. Fractal characteristics for coal chemical structure: Principle, methodology and implication. *Chaos Solitons Fractals* **2023**, *173*, 113699. [CrossRef]
25. Zhang, J.; Ni, X.; Heng, S.; Wu, L. Influences of acidic solvents on changes in microstructure and adsorptive properties of lean coal. *J. Mol. Struct.* **2024**, *1318*, 139245. [CrossRef]
26. Dong, K.; Zhong, D.; Lu, Y.; Yan, J.; Dai, W. Facilitating desorption and diffusion of coalbed methane by wetting-corrosion: Perspectives from the change of pore structure. *Gas Sci. Eng.* **2023**, *119*, 205138. [CrossRef]
27. Zhang, J.; Ni, X.; Su, E.; Liu, X. Simulation of the influences of different minerals contained in acidified coal on CH_4 adsorption. *J. Mol. Struct.* **2023**, *1294*, 136328. [CrossRef]
28. Dou, H.; Xie, J.; Xie, J.; Sun, G.; Li, Z.; Wang, Z.; Miao, Y. Study on the mechanism of the influence of HNO_3 and HF acid treatment on the CO_2 adsorption and desorption characteristics of coal. *Fuel* **2022**, *309*, 122187. [CrossRef]
29. Wang, Y.; Mei, F.; Xue, S. Comparative analysis of microstructure evolution and oxidation performance of acid-treated lignite. *Fuel Process. Technol.* **2021**, *215*, 106750. [CrossRef]
30. Yi, Z.; Yuannan, Z.; Bingyou, J.; Guofeng, Y.; Bo, R.; Changfei, Y.; Shiju, W. Experimental study on the influence of acid fracturing fluid on coal wettability. *Fuel* **2023**, *343*, 127965.
31. Jiang, B.; Zhang, Y.; Zheng, Y.; Yu, C.; Wang, S.; Lin, H.; Lu, K.; Ren, B.; Nie, W.; Yu, H.; et al. Effect of acid-thermal coupling on the chemical structure and wettability of coal: An experimental study. *Energy* **2024**, *294*, 130943. [CrossRef]
32. Ni, G.; Li, S.; Rahman, S.; Xun, M.; Wang, H.; Xu, Y.; Xie, H. Effect of nitric acid on the pore structure and fractal characteristics of coal based on the low-temperature nitrogen adsorption method. *Powder Technol.* **2020**, *367*, 506–516. [CrossRef]

33. Su, J.; Zhuo, X.; Zhang, L.; Wang, L.; Guo, M.; Zhang, B.; Li, M.; Ni, Z. Efficient removal behaviors and correlation rules of Na from Zhundong coal with low concentration organic acids. *Fuel* **2023**, *350*, 128803. [CrossRef]
34. Yu, Y.; Xing, H.; Cheng, W.; Cui, W.; Chen, Y. Microstructure evolution law and dissolution time effect of bituminous coal under acetic acid acidification: Based on Micro-CT image analysis. *Fuel* **2024**, *359*, 130392. [CrossRef]
35. Lu, J.; Zheng, C.; Liu, W.; Li, H.; Shi, S.; Lu, Y.; Ye, Q.; Zheng, Y. Evolution of the pore structure and fractal characteristics of coal under microwave-assisted acidification. *Fuel* **2023**, *347*, 128500. [CrossRef]
36. Mohsen, M.; Hamed, A.; Yang, Y.; Faisal Ur Rahman, A.; Stefan, L.; Maxim, L.; Alireza, K. Coal cleat network stimulation through a combination of acidizing and liquid nitrogen fracturing. *Gas Sci. Eng.* **2024**, *125*, 205308.
37. Xun, M.; Xie, J.; Xie, J.; Sun, Q.; Lu, S.; Wang, G. Study on the effect of acid-heat coupling on the damage characteristics of coal pore-fissure structure. *Adv. Powder Technol.* **2021**, *32*, 3425–3435. [CrossRef]
38. Su, C.; Tan, B.; Jiang, Y.A.; Song, X.Z.; Shao, Z.Z.; Liu, B.; Gao, L.Y.; Wang, H.Y. Study on the influence of different acid and alkali environments on the spontaneous combustion properties of coal. *Energy* **2024**, *293*, 130525. [CrossRef]
39. Li, X.W.; Li, X.C.; Chen, Z.F.; Zeng, J.H.; Zhang, S.H.; Shi, Y.Y.; Li, Z.B.; Zhang, Q.; Nie, B.S.; Chen, X.L. Macro-Meso-Micro Evolution Characteristics of Coal Under Acid Corrosion and Its Implication to ECBM Recovery. *Energ Fuel* **2024**, *38*, 22205–22218. [CrossRef]
40. Chen, S.Y.; Li, Z.S.; Liang, M.J.; Tan, S.H.; Shi, Y.P.; Chen, Z.X.; Yang, X.Y.; Cai, J.H. Mechanisms of Acid- and Chelating Agent-Induced Coal Permeability Response Considering the Stress Sensitivity Effect. *Energ Fuel* **2022**, *36*, 14812–14823. [CrossRef]
41. Wang, H.; Cheng, X.; Tian, J.; Li, T.; Wang, W.; Pan, J.; Niu, Q.; Feng, S.; Hao, H.; Zhang, Y. Permeability enhancement of low rank coal through acidization using H2S solution: An experimental study in the Kuqa-Bay Coalfield, Xinjiang, China. *J. Petrol. Sci. Eng.* **2020**, *185*, 106476. [CrossRef]
42. Wang, L.; Liu, M.; Zhao, Y.; Liao, X.; Li, J.; Zhao, Z.; Liu, Q. Multi-scale pore structure transformation of shale under mixed acid acidification method. *Arab. J. Chem.* **2023**, *16*, 104937. [CrossRef]
43. Guo, H.; Yuan, L.; Cheng, Y.; Wang, K.; Xu, C. Experimental investigation on coal pore and fracture characteristics based on fractal theory. *Powder Technol.* **2019**, *346*, 341–349. [CrossRef]
44. Zhang, Z.; Liu, G.; Wang, X.; Lv, R.; Liu, H.; Lin, J.; Barakos, G.; Chang, P. A fractal Langmuir adsorption equation on coal: Principle, methodology and implication. *Chem. Eng. J.* **2024**, *488*, 150869. [CrossRef]
45. Zhang, Z.; Liu, G.; Lin, J.; Barakos, G.; Chang, P. Fractal Evolution Characteristics on the Three-Dimensional Fractures in Coal Induced by CO_2 Phase Transition Fracturing. *Fractal Fract.* **2024**, *8*, 273. [CrossRef]
46. Feng, K.; Liu, G.; Zhang, Z.; Liu, H.; Lv, R.; Wang, X.; Chang, P.; Lin, J.; Barakos, G. Fractal Strategy for Improving Characterization of N_2 Adsorption–Desorption in Mesopores. *Fractal. Fract.* **2024**, *8*, 617. [CrossRef]
47. Zhang, L.J.; Li, Z.H.; Yang, Y.L.; Zhou, Y.B.; Kong, B.; Li, J.H.; Si, L.L. Effect of acid treatment on the characteristics and structures of high-sulfur bituminous coal. *Fuel* **2016**, *184*, 418–429. [CrossRef]
48. *GB/T 216503-2011*; Determination of Pore Size Distribution and Porosity of Solid Materials by Mercury Intrusion and Gas Adsorption. National Technical Committee for the Standardization of Methods for Screening and Particle Sorting: Beijing, China, 2011.
49. *SY/T 5163-2018*; Analysis Methodfor Clay Minerals and Ordinary Non- Clay Minerals in Sedimentary Rocks by the X-Ray Diffraction. National Energy Administration: Beijing, China, 2019.

Disclaimer/Publisher's Note: The statements, opinions and data contained in all publications are solely those of the individual author(s) and contributor(s) and not of MDPI and/or the editor(s). MDPI and/or the editor(s) disclaim responsibility for any injury to people or property resulting from any ideas, methods, instructions or products referred to in the content.